Effect of Magnetic Interactions on Magnetic Remanence in a Fine Particle System

Sauviz P. Alaei and E. Dan Dahlberg

School of Physics and Astronomy, University of Minnesota, Minneapolis, MN 55455 USA

The magnetic field-dependent remanent magnetization and demagnetization of magnetite nanoparticles dispersed in a frozen isoparaffin oil have been measured as a function of magnetite concentration. Frozen ferrofluid samples with magnetite volume fractions between 7.1% and 0.03% were demagnetized using either thermal or dc demagnetization and were kept frozen at 77 or 4 K during measurement to restrict mechanical rotation and translation of the particles. The magnetization and demagnetization remanences of the frozen ferrofluid were measured and plotted parametrically in the magnetic field magnitude to produce Henkel and ΔM plots for comparison with the Wohlfarth model. The Henkel and ΔM plots of the ferrofluid samples with higher concentrations of magnetite deviated from the predictions of the Wohlfarth non-interacting model, consistent with demagnetizing interactions in the system. The magnitude of this deviation decreased with decreasing magnetite concentration. A simple model is presented that quantitatively explains the deviations from the expected relations and can be used in other systems to characterize magnetic interactions.

Index Terms—**Henkel plot, magnetic nanoparticles, magnetic remanence, Wohlfarth model.**

I. Introduction

THE Wohlfarth model [1] describes the remanent magnetic behavior of a system of single domain, non-interacting magnetic particles with uniaxial magnetic anisotropy. Wohlfarth [1] compared two magnetization paths, the first starting from a demagnetized state and the other starting from the remanent state following application of a saturating magnetic field. He calculated the relationship between the magnetization remanence, $M_r(H)$, after application of a magnetic field, H, and the demagnetization remanence, $M_d(H)$, for the same H, normalized to the remanence after application of a saturating magnetic field. He considered three processes to produce the zero magnetization state: the first is thermal or ac demagnetization and it is the one most researchers exploit. It is achieved by randomly orienting the individual dipole moments of each particle, thus resulting in net zero magnetization. In this case, the so-called Wohlfarth relation between M_d and M_r for a thermally demagnetized, non-interacting system is [1]

$$M_d(H) = 1 - 2M_r(H). \tag{1}$$

Both the second and third demagnetization methods involve applying a saturating dc magnetic field followed by a reverse dc magnetic field, H_0, that produces a zero magnetization state in zero field. These two methods differ only in the direction of the initial saturating field. In one case, called dc backward (DCB) demagnetization,[1] the initial saturating field is applied in the "negative" direction (where the "positive" direction is the direction we choose to apply the fields when measuring M_r). The normalized Wohlfarth relation for a DCB demagnetized, non-interacting system is [2]

$$M_r^{DCB}(H) = \begin{cases} 0, & H < H_0 \\ -M_d(H), & H > H_0. \end{cases} \tag{2}$$

The third method, called dc forward (DCF) demagnetization, is the opposite case in which the initial saturating field is applied in the positive direction (the same direction in which we apply fields to measure M_r). The normalized Wohlfarth relation for a DCF demagnetized, non-interacting system is [2]

$$M_r^{DCF}(H) = \begin{cases} 1 - M_d(H), & H < H_0 \\ 1, & H > H_0. \end{cases} \tag{3}$$

A diagram illustrating the DCB and DCF demagnetization processes is included in Appendix A. Note that the definition (and measurement protocol) of M_r and M_d is identical in all three cases and is depicted in Appendix B for clarity. The difference in (1)–(3) arises from different paths to the initial demagnetized state. However, the demagnetization remanence is invariant between all three cases, as its measurement always starts from a saturated system. The relations in (1)–(3) are easily seen when the normalized magnetization and demagnetization remanences are plotted parametrically in field magnitude, in what is known as a Henkel plot [3]. Furthermore, the relation specific to thermally demagnetized systems is often examined using the quantity ΔM given by [4]

$$\Delta M(H) = M_d(H) - [1 - 2M_r(H)] \tag{4}$$

which quantifies the deviation from (1).

This model finds applications in the study of particulate recording media [5]–[7] and, more generally, the characterization of materials [8]–[11]. Previous attempts to observe the behavior of the magnetic remanence in various thermally demagnetized systems, such as magnetic tape [6], [7] and other magnetic materials [3], [9]–[11], have shown the measured remanences deviating from the relationship predicted by the

Manuscript received 28 November 2021; revised 31 March 2022; accepted 20 May 2022. Date of publication 25 May 2022; date of current version 26 July 2022. Corresponding author: S. P. Alaei (e-mail: alaei005@umn.edu).

Color versions of one or more figures in this article are available at https://doi.org/10.1109/TMAG.2022.3177807.

Digital Object Identifier 10.1109/TMAG.2022.3177807

[1] $M_r(H)$ and $M_d(H)$ are sometimes referred to as the isothermal remanent magnetization (IRM) and direct current demagnetization (DCD), respectively. Note that DCB and DCF are protocols used to demagnetize a system, not to be confused with the DCD.

Wohlfarth model. The disagreements with theory in these cases have been attributed to interactions between magnetic particles or domains in the system, and the initial state not being statistically random, which is a condition explicitly required by the Wohlfarth model for thermal demagnetization. Simulations have shown these to be feasible explanations [12]. Similarly, deviations from the Wohlfarth model have been seen for DCF demagnetized systems [10] and were also attributed to interactions in the system.

In our investigation, we have tested the Wohlfarth model by creating a system of magnetic particles that can be thermally demagnetized easily. As stated above, the latter condition has been difficult to produce in previous studies; we achieved this using a ferrofluid [13] consisting of magnetite nanoparticles with a narrow size distribution uniformly dispersed in an isoparaffin oil. We have systematically varied the interactions between these particles by diluting the original ferrofluid with additional isoparaffin oil [14], thus increasing the average particle separation. For the most dilute samples at 77 K, we have reached the non-interacting limit in agreement with Wohlfarth's model for all three demagnetization processes used. Furthermore, we present a simple model to account for interactions observed in the ferrofluid samples with higher particle concentration. The model provides a quantitative analysis process for the use of Henkel or ΔM plots to determine the net interactions in a system as a function of the applied magnetic field.

II. Theory

Wohlfarth's original work [1] did not include a derivation of the relations between M_{r} and M_{d}, nor have many subsequent works that make use of the result. An in-depth derivation of (1)–(3) is found in [2], but here we provide a more concise derivation of (1) using a simple model system. This model system consists of a collection of identical, non-interacting magnetic particles with uniaxial magnetic anisotropy. Taking a random direction, $\hat{Z}$, for the direction of the applied magnetic field, the magnetization remanence, $M_{\mathrm{r}}(H)$, is defined as the $\hat{Z}$ component of the zero-field magnetization of a system following the application and subsequent removal of a dc magnetic field, H. Similarly, the demagnetization remanence, $M_{\mathrm{d}}(H)$, is the $\hat{Z}$ component of the zero-field magnetization of a system following saturation in the $\hat{Z}$-direction and the application and removal of a field, H, in the $-\hat{Z}$-direction.

When this system is thermally demagnetized, the dipole moment, $\overrightarrow{\mu}$, for each particle is aligned with its respective easy axis, and the easy axes of all the particles are randomly oriented, thus resulting in a net magnetic moment of zero in the absence of an external field. A randomly selected magnetic particle has an easy axis that makes an angle θ with the $\hat{Z}$-axis. Upon application of a dc magnetic field in the $\hat{Z}$-direction, the dipole moment $\overrightarrow{\mu}$ will rotate toward the applied field direction, to an extent dependent on field magnitude and anisotropy energy. When this field is removed, $\overrightarrow{\mu}$ will return to pointing along its easy axis; the direction that it points along the easy axis will be whichever of the two directions that made a smaller angle with $\overrightarrow{\mu}$ when the field was applied. If this results in a reversal of the initial zero field direction, then the moment has switched. The minimum field component in the $\hat{Z}$-direction that is required to switch $\overrightarrow{\mu}$ will be referred to as the "switching field," denoted by H_{sf}. A given particle's contribution to the magnetization in the $\hat{Z}$-direction will equal $\mu\cos(\theta)$, where $\mu = |\overrightarrow{\mu}|$.

Each particle in our system of non-interacting uniaxially anisotropic magnetic particles has the same magnetic moment, μ, and the same anisotropy energy, but all are randomly oriented. Thus, for each particle, the switching field depends only on θ, the relative angle between a particle's easy axis and $\hat{Z}$. That is,

$$H_{\mathrm{sf}} = H_{\mathrm{sf}}(\theta). \tag{5}$$

For a given field of magnitude H_n, suppose we have k_n dipoles for which this field is the switching field. Equation (5) implies that all k_n dipoles will have an easy axis with the same discrete relative angle to $\hat{Z}$, called θ_n, and thus,

$$k_n = k_n(\theta_n). \tag{6}$$

We may now recursively define the magnetization remanence, M_{r}, of this system starting from a thermally demagnetized state as a function of the applied field, H_n, in the $\hat{Z}$-direction (with the further condition that H_{n} increases monotonically with n)

$$M_{\mathrm{r}}(H_n) = M_{\mathrm{r}}(H_{n-1}) + \frac{1}{2}k_n \cdot \mu\cos(\theta_n)$$

with

$$M_{\mathrm{r}}(H_0) \equiv M_{\mathrm{r}}(0) = 0. \tag{7}$$

Note that the addition to the remanent magnetization in going from a field H_{n-1} to H_n is only half the total moment (in the $\hat{Z}$-direction) of all k_n dipoles. This is because the thermally demagnetized system is initially in a statistically random starting state, in which half of the dipoles already satisfy $\overrightarrow{\mu} \cdot \hat{Z} > 0$. The randomness ensures that such dipoles are distributed uniformly across each set of k_n dipoles, meaning that half of each k_n will already be pointing in the positive $\hat{Z}$-direction and the application of H_n only switches the other half. We may express (7) more compactly as

$$M_{\mathrm{r}}(H_n) = \frac{1}{2}\sum_{i=1}^{n} k_i \cdot \mu\cos(\theta_i). \tag{8}$$

With a sufficiently large field, all dipoles will switch to the $\hat{Z}$-direction, and the system will have reached its saturation remanence, $M_{\mathrm{R}}(\infty)$. We may then define the demagnetization remanence, M_{d}, in a similar fashion, where the field H_n is applied in the $-\hat{Z}$-direction and now switches all k_n dipoles

$$M_{\mathrm{d}}(H_n) = M_{\mathrm{d}}(H_{n-1}) - k_n \cdot \mu\cos(\theta_n)$$

with

$$M_{\mathrm{d}}(H_0) \equiv M_{\mathrm{d}}(0) = M_{\mathrm{r}}(\infty). \tag{9}$$

Or, more compactly

$$M_{\mathrm{d}}(H_n) = M_{\mathrm{r}}(\infty) - \sum_{i=1}^{n} k_i \cdot \mu\cos(\theta_i). \tag{10}$$

Noting that the summation term is twice that of (8), we see the Wohlfarth relation for a thermally demagnetized system

$$M_{\mathrm{d}}(H) = M_{\mathrm{r}}(\infty) - 2M_{\mathrm{r}}(H). \tag{11}$$

Normalizing (11) by the saturation remanence, $M_{\mathrm{r}}(\infty)$, we recover (1).

A similar analysis, omitted here, produces the other two Wohlfarth relations, (2) and (3), for dc demagnetized systems.

III. Experimental Setup and Methods

The samples used over the course of this study were based on a commercially available ferrofluid [13] consisting of isoparaffin oil with varying concentrations of 10 nm-diameter magnetite nanoparticles with a narrow size distribution. The samples were prepared from the same batch of original ferrofluid and diluted with additional isoparaffin oil [14] to alter particle concentration.

A. Measurements at 4 K

The five samples used for measurements at 4 K had magnetite volume fractions of 7.1% (the undiluted ferrofluid), 1.4%, 0.7%, 0.3%, and 0.03%. Samples were prepared in glass nuclear magnetic resonance (NMR) tubes (Wilmad 507-PP 8 in), which were sealed under a rough vacuum of approximately 160 mmHg. Each sample contained 1–30 μL of the undiluted ferrofluid. The magnetization and demagnetization remanences were measured with a Magnetic Property Measurement System 3 (MPMS 3) [15] in dc measurement mode. To prevent magnetization by mechanical rotation, measurements were made with the samples frozen at 4 K. This ensured that the particles could not rotate or translate within the isoparaffin oil. For thermal demagnetization, the samples were brought to 300 K and then cooled to 4 K in zero field; the magnet of the MPMS 3 was quenched prior to cooling the sample, to ensure no remanent field was present. For the DCB and DCF demagnetized states, the ferrofluid was frozen at 4 K and demagnetized using the respective protocol described in Section I and Appendix A.

Starting from one of the three demagnetized states in zero magnetic field, dc magnetic fields were applied to the frozen ferrofluid, increasing in increments between 0 and 2500 Oe. Following each increment, the field was removed and the zero-field magnetic moment, equal to the magnetization remanence, M_{r}, was measured. This process continued until saturation of the remanence at approximately 2500 Oe. From the saturated state, the magnetic field polarity was reversed and the process was repeated for the same magnetic field magnitudes, now measuring the demagnetization remanence, M_{d}, for each field. The final dataset was normalized by the magnetization remanence measured at saturation. Throughout the entire process, the sample remained frozen at 4 K.

B. Measurements at 77 K

The 14 samples used for measurements at 77 K had one of the four volume fractions of magnetite: 7.1% (the undiluted ferrofluid), 2.5%, 1.4%, and 0.7%. Samples were prepared in a size 5 gelatin pill capsule and nominally contained 10 μL of the undiluted ferrofluid. The magnetization and demagnetization remanences were measured using a vibrating sample magnetometer (VSM) [16]. Although room temperature was sufficient to thermally demagnetize the samples, providing a statistically random initial state, samples were sonicated on occasion to ensure randomness; there were no discernable differences in the results of these measurements. Measurements were made following the same process described above, but with a maximum applied field of 400 Oe, at which point the magnetization was saturated at 77 K.

The measurement protocol at 77 K was repeated multiple times for samples of each volume fraction to obtain an average normalized $M_{\mathrm{r}}(H)$ and $M_{\mathrm{d}}(H)$ for each demagnetization method. Note that samples with the same magnetite concentration produced, within the experimental uncertainty, the same results, i.e., the physics was consistent for all measurements from different samples with the same concentration of particles. The total number of VSM measurements that were averaged varied for different ferrofluid concentrations, but ranged between 25 and 31 measurements for thermal demagnetization data, 13 and 17 for DCB data, and 12 and 17 for DCF data. The values of $M_{\mathrm{d}}(H)$ reported here were averaged over all measurements made using all three demagnetization methods, as it is invariant of the initial demagnetization process. The average normalized remanences were then plotted parametrically in field magnitude to obtain Henkel plots for each sample.

IV. Results and Discussion

A. Henkel and ΔM Plots at 4 K

Fig. 1 shows the normalized Henkel plots at 4 K for each measured volume fraction. There are four key features present in the data. The first is the shift of the Henkel plot downward and to the left relative to the Wohlfarth relation, (1), for the thermally demagnetized starting state. Second, similar to the first, is the shift of the Henkel plot downward and to the left relative to the Wohlfarth relation, (3), for the DCF demagnetized starting state. The third feature is the invariance of the Henkel plot for DCB demagnetization across all particle concentrations, and the fourth feature is the convergence of the Henkel plots to the Wohlfarth relations with decreased particle concentration.

Regarding the deviation of the thermal demagnetization data from the Wohlfarth relation, previous research [6], [10], [11] has found a similar nonlinear relationship between M_{d} and M_{r} in a variety of thermally demagnetized systems in which the Henkel plot is shifted downward and to the left relative to the Wohlfarth relation. In these works, the deviation was attributed to interactions that tend to demagnetize the system, and simulations have yielded similar Henkel plots for thermally demagnetized systems of uniaxial particles interacting only through dipolar interactions [12]. As a brief illustration of the importance of the dipolar interaction and its tendency to be demagnetizing, we consider the case of a uniformly magnetized distribution of dipoles aligned along the same direction in Appendix C. The attribution of the disagreement

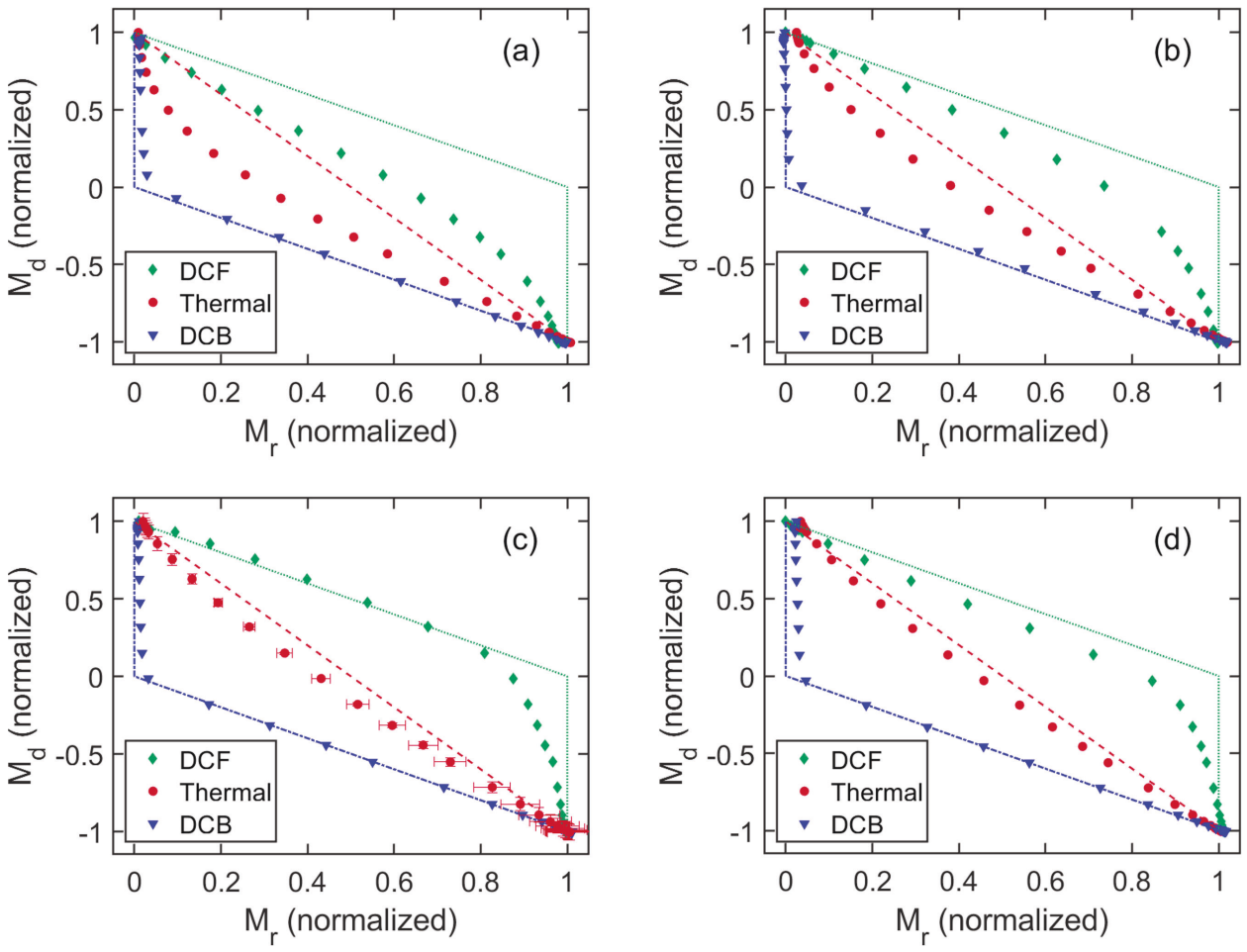

Fig. 1. Henkel plots at 4 K for magnetite volume fractions of: (a) 7.1%; (b) 0.7%; (c) 0.3%; and (d) 0.03%. A representative sample of the vertical and horizontal error bars is seen in the thermal data of (c). Measurements were made with an MPMS 3 [15] in dc measurement mode. For each sample, the saturation remanence was approximately 0.40 of the saturation magnetization. The red dashed line is (1), the blue dash-dotted curve is (2), and the green dotted curve is (3).

with the Wohlfarth model to interactions in the system may be carefully extended to the DCF data, as was done in [10], but it is clear from Fig. 1 that DCB demagnetized systems require a more detailed analysis.

The invariance of the Henkel plots for DCB demagnetization is consistent with previous work [10] and can be explained here by considering the initial state of the DCB demagnetized frozen ferrofluid. In the DCB process, the saturating negative field aligns all individual dipoles in the negative direction, and the demagnetizing positive field, H_0, switches only the "easy" dipoles (those that can be switched with weaker fields) to the positive direction. Thus, measurement of the magnetization remanence of a DCB demagnetized system involves switching only the "hard" dipoles, which require stronger fields to switch and are less susceptible to magnetic fields from nearby interacting particles. This reasoning is also consistent with the fact that interactions are clearly observed in DCF and thermally demagnetized Henkel plots. The DCF process is the opposite of DCB, and measurement of the magnetization remanence involves switching the easy (rather than hard) dipoles, which are most affected by magnetic fields from nearby interacting particles. Meanwhile, in a thermally demagnetized system, both easy and hard dipoles are switched when measuring

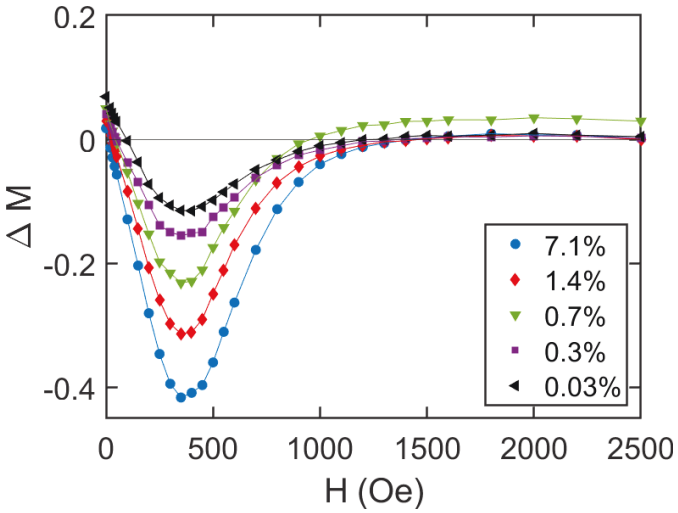

Fig. 2. ΔM plots at 4 K for each magnetite volume fraction, calculated for the thermal demagnetization data of Fig. 1. Error bars omitted for clarity.

the magnetization remanence, which places its sensitivity to interactions between the extremes of DCF and DCB.

The final feature in Fig. 1, the convergence of the Henkel plots to the Wohlfarth relations with decreased particle

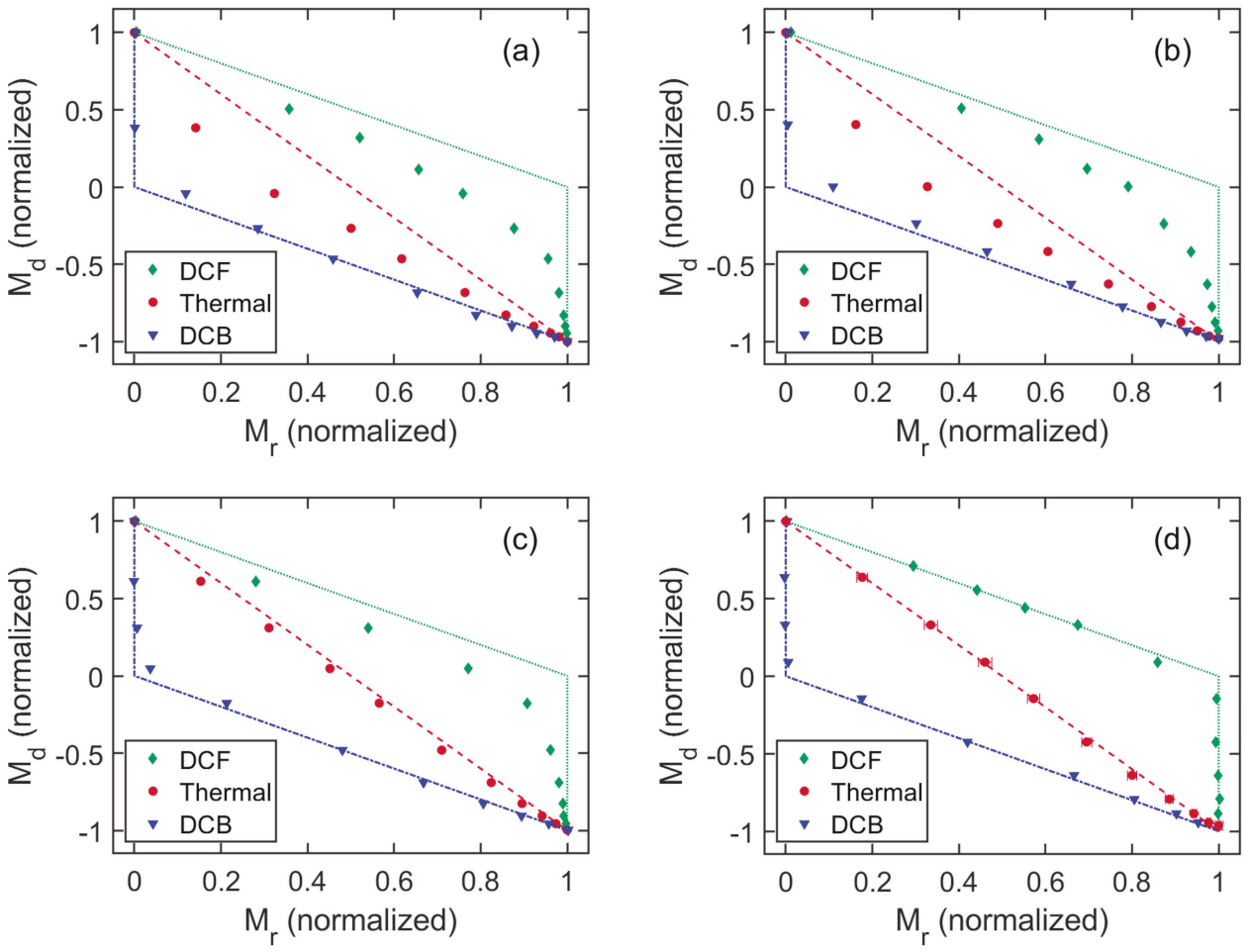

Fig. 3. Henkel plots at 77 K for magnetite volume fractions of: (a) 7.1%; (b) 2.5%; (c) 1.4%; and (d) 0.7%, measured with a VSM [16]. A representative sample of the vertical and horizontal error bars, equal to the standard error, is seen in the thermal data of (d). The maximum standard error across all normalized data points at 77 K was 0.03. The saturation remanence was approximately 0.075 of the saturation magnetization for each sample. The red dashed line is (1), the blue dash-dotted curve is (2), and the green dotted curve is (3).

concentration, can be explained by considering the relative strength of interactions in each of the samples. This trend is most clearly illustrated for the thermal demagnetization data and can be examined using the quantity ΔM given by (4).

Fig. 2 shows the ΔM plots for each volume fraction. Recall that decreasing the magnetite particle concentration increases the average separation between particles; this separation scales as the inverse cube-root of particle concentration, while the strength of the dipolar magnetic field scales as the inverse cube of distance. Thus, we expect the strength of the dipolar interactions to scale with the particle concentration. However, it is not clear where this proportionality is represented in the ΔM plot, and we note that the relationship between peak observed ΔM and volume fraction was not linear. Nevertheless, it is clear that a decrease in magnetite volume fraction results in weaker magnetic interactions and, thus, better agreement with the Wohlfarth model. This explanation is consistent with simulations of particulate systems [12], in which Henkel plots of thermally demagnetized systems with varying interaction strengths are compared and show the same trend seen in Fig. 2.

A final comment regarding the results at 4 K is as follows: a hysteresis loop measurement found a maximum remanent magnetization of 0.43 of the saturation magnetization. For randomly distributed, non-interacting particles in three dimensions, we would expect a value of 0.5 [2]. We attribute this discrepancy to some clustering of the particles; we also attribute this clustering to be responsible for the deviations in the Henkel and ΔM plot for the most dilute sample.

B. Henkel Plots at 77 K

Fig. 3 shows the normalized Henkel plots at 77 K for each measured volume fraction. Once again we observe the same four features described in Section IV-A, which are explained by the same reasoning provided there. The corresponding ΔM plots are omitted but show the same trend as Fig. 2. It is interesting to note that agreement with the Wohlfarth model occurs with a magnetite volume fraction of 0.7% at 77 K, but not at 4 K, as shown in Fig. 1(b). We attribute this to many of the particles being superparamagnetic at 77 K [17]. This is further supported by a hysteresis loop at 77 K that shows a maximum remanence of less than 0.1 of the saturation magnetization rather than 0.5 expected [2]. An analysis of the Henkel plots, similar to that performed for the 4 K data, yields similar results, and is, therefore, omitted here.

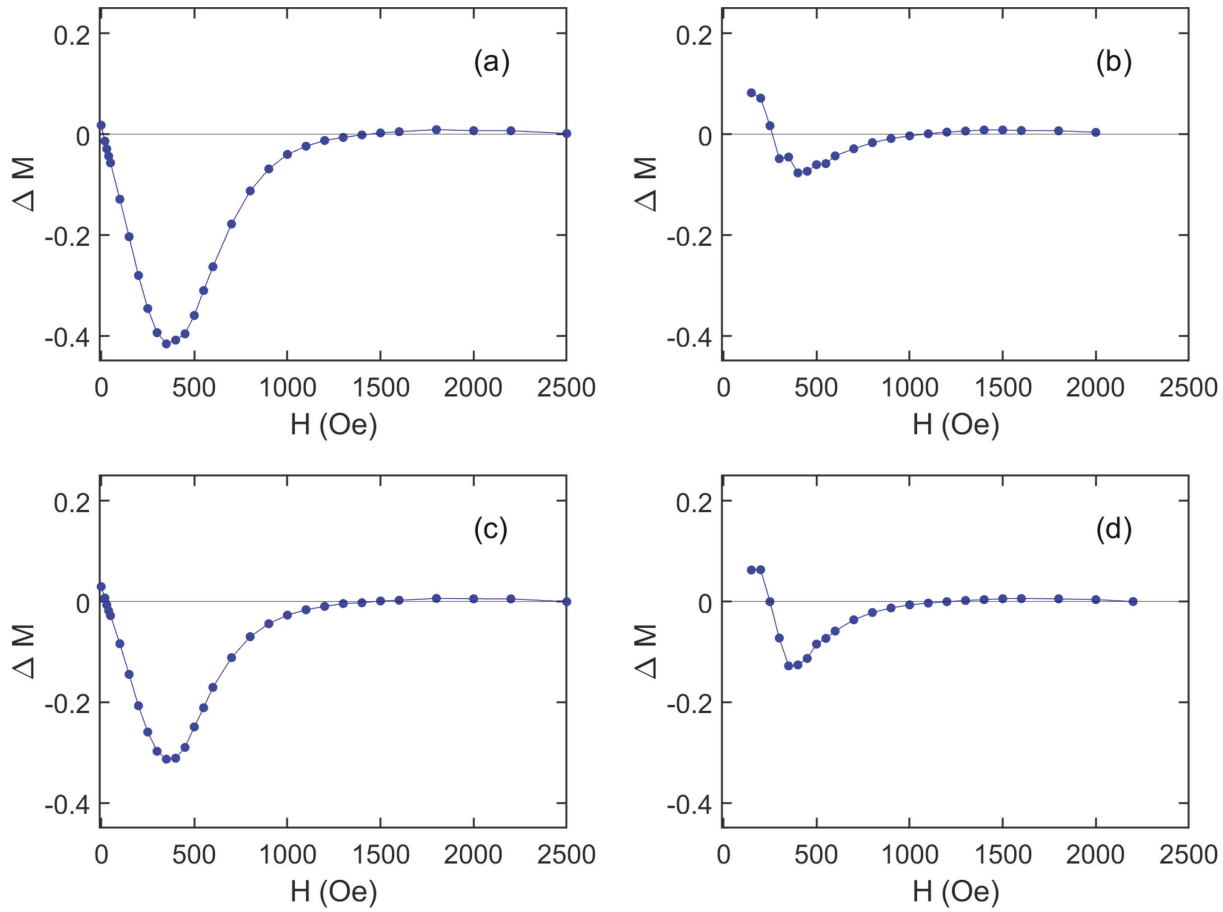

Fig. 4. Uncorrected (left) and corrected (right) ΔM plots for thermally demagnetized samples with magnetite volume fractions of: (a) and (b) 7.1% and (c) and (d) 1.4%. See Appendix D for the corresponding Henkel plots. The value of α was 0.85 for the top row and 4.0 for the bottom row.

C. Modeling Interactions

To account for the demagnetizing interactions in the system, we propose an effective field, $\vec{\boldsymbol{H}}_{eff}$, felt by the particles in the ferrofluid given by

$$\vec{\boldsymbol{H}}_{eff} = \vec{\boldsymbol{H}} - \alpha \vec{\boldsymbol{M}}(H) \tag{12}$$

where $\vec{\boldsymbol{H}}$ is the applied field, $\vec{\boldsymbol{M}}(H)$ is the magnetization of the system measured with the field applied, and α is a unitless constant dependent on the geometry and other magnetic properties of the system. The second term accounts for the net interactions in the system, which are demagnetizing in the case of positive α. This model suggests that when initially magnetizing the sample in the defined positive direction, $\hat{Z}$, the applied field magnitude is decreased by $\alpha M(H)$ (since $\vec{\boldsymbol{H}}$ and $\vec{\boldsymbol{M}}$ are parallel). Thus, the effective field magnitude is

$$H_{\text{eff}} = H - \alpha M(H) \text{ (for magnetization)} \tag{13}$$

where we have used $H \equiv |\vec{\boldsymbol{H}}|$ and $M \equiv \hat{Z} \cdot \vec{\boldsymbol{M}}$.

When demagnetizing the system (after saturation in the positive direction), we apply the field in the negative direction but, for fields weaker than the coercivity, $\vec{\boldsymbol{M}}$ continues to point in the positive direction. In this case, according to (12), the applied field magnitude is increased by $\alpha M(-H)$, and the effective field magnitude is given by

$$H_{\text{eff}} = H + \alpha M(-H) \text{ (for demagnetization).} \tag{14}$$

Notice that (14) still holds for applied fields in the negative direction stronger than the coercivity, where we would have $M < 0$, in which case (14) is equivalent to (13) in the sense that $H_{\text{eff}} < H$.

Because the data were taken in set field increments, corrected values for $M_{\text{r}}(H)$ and $M_{\text{d}}(H)$ were obtained by performing a linear interpolation of $M_{\text{r}}(H - \alpha M)$ and $M_{\text{d}}(H + \alpha M)$, respectively. In applying the corrections to our data, we treated α as a fitting parameter, and selected the value which resulted in the best agreement of the corrected Henkel plot with the Wohlfarth model. This analysis was performed for all five samples measured at 4 K, but for brevity, we only present the corrected plots for two samples here.

Fig. 4 shows the effect of the corrections detailed above on the two most interacting samples measured at 4 K, with volume fractions of 7.1% and 1.4%. In comparing the uncorrected ΔM plots, Fig. 4(a) and (c), with the corrected plots in Fig. 4(b) and (d), respectively, we see that the strong deviations shown in the uncorrected plots, due to demagnetizing interactions, are no longer as apparent in the corrected plots. The best-fitting values for α are consistent with being dominated by the nearest neighbor distance, as might be expected with

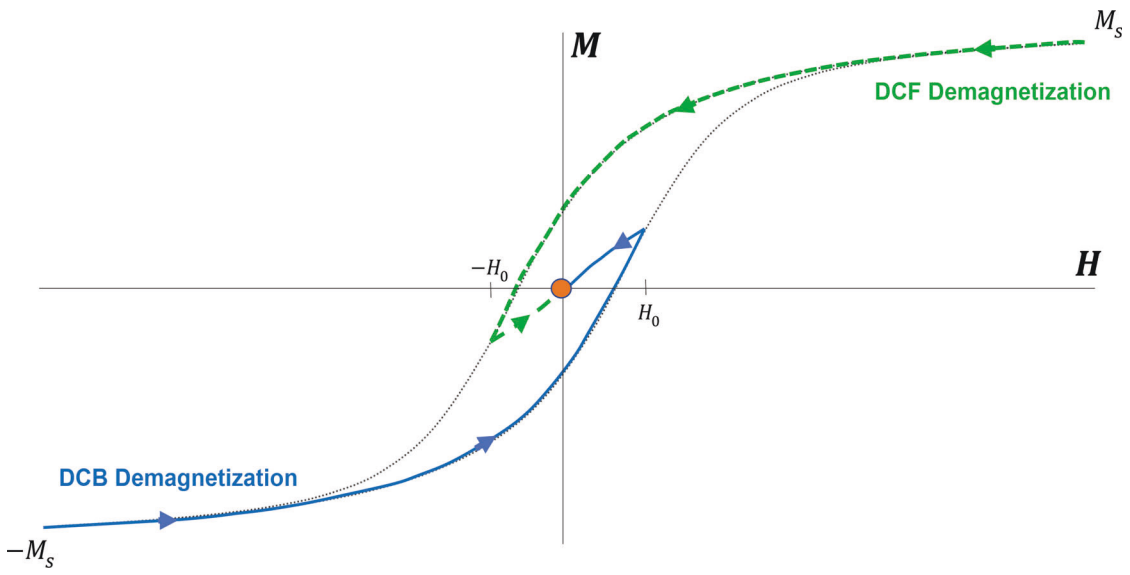

Fig. 5. Diagram of the DCF and DCB demagnetization processes.

a simple Lorentz field analysis [18]. The corrected ΔM plots show good agreement with the Wohlfarth model, except at low fields; the corrected Henkel plots are in Appendix D.

The low field deviations in our corrected ΔM plots (Fig. 4(b) and (d), and plots for the other samples that are not shown) are an artifact resulting from the magnet's remanent field. The demagnetization remanence measurements are made immediately following the application of a stronger, saturating magnetic field in the positive direction. Thus, when measuring the demagnetization remanence, there is a remanent field initially pointing in the positive direction, that later points in the negative direction after sufficiently large negative fields are applied in the reversal process. So our values of M_{d} are initially overestimated and then underestimated, as reflected in the corrected plots. Values of M_{r} at low fields are unaffected since the magnet was quenched prior to measurement.

V. Conclusion

The effect of magnetite nanoparticle concentration on the magnetic remanence of a fine particle system has been investigated in frozen ferrofluids with magnetite volume fractions between 7.1% and 0.03%. The Henkel plots for samples with greater volume fraction showed net demagnetizing interactions in the ferrofluid and deviated from the non-interacting Wohlfarth model. As expected, the magnitude of the deviation decreased with decreasing magnetite concentration, consistent with the weakening of interactions in the system. Most importantly, this study provides a path for the use of the Henkel or ΔM plots to determine and quantitatively model the net interactions in a general system.

Appendix A

The dc demagnetization processes are illustrated in Fig. 5. In the DCF process (green dashed), a saturating field is applied in the positive direction followed by a zeroing field, H_0, in the negative direction. In the DCB process (blue solid), the saturating field is applied in the negative direction followed by a positive zeroing field. Both processes end at an $M = 0$ state in zero field, marked with the orange dot, from which measurement of the magnetization remanence begins. The remanence measurement is done with $M_{\mathrm{r}}(H)$ being measured for H applied in the positive direction, as shown in Appendix B.

Appendix B

The zero-field intercept of the solid curve in Fig. 6 is $M_{\mathrm{r}}(H)$, and the zero-field intercept of the dashed curve is $M_{\mathrm{d}}(H)$.

Appendix C
Mean Field From a Magnetic Dipole

The magnetic field from a pure dipole of magnitude $m > 0$ directed along the $+\hat{z}$-axis is given by

$$\vec{B}(r,\theta) = \frac{\mu_0 m}{4\pi r^3}(2\cos(\theta)\hat{r} + \sin(\theta)\hat{\theta}) \tag{A1}$$

where r is the radial distance and θ is the polar angle of spherical coordinates. A neighboring dipole will experience a ferromagnetic interaction when $B_z \equiv \vec{B} \cdot \hat{z} > 0$ and an antiferromagnetic interaction when $B_z < 0$. For spherical coordinates, $\hat{z}$ is given by

$$\hat{z} = \cos(\theta)\hat{r} - \sin(\theta)\hat{\theta}. \tag{A2}$$

And so

$$B_z(r,\theta) = \frac{\mu_0 m}{4\pi r^3}\left(2\cos^2(\theta) - \sin^2(\theta)\right). \tag{A3}$$

Now consider a spherical shell of arbitrary radius R. Say we have N dipoles uniformly distributed along its surface. Within a ring on this spherical surface, with constant θ and infinitesimal thickness, we will have dN dipoles

$$dN(\theta) = \frac{N}{4\pi R^2} \cdot 2\pi R\sin(\theta) \cdot R\sin(\theta)d\theta. \tag{A4}$$

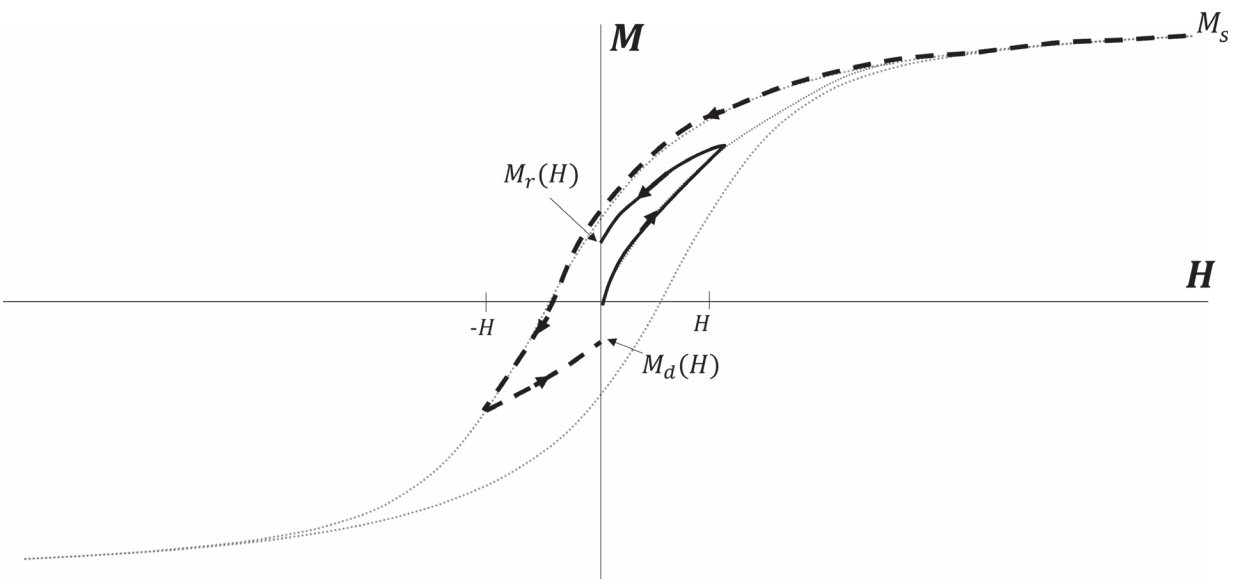

Fig. 6. Graphical representation of M_r and M_d.

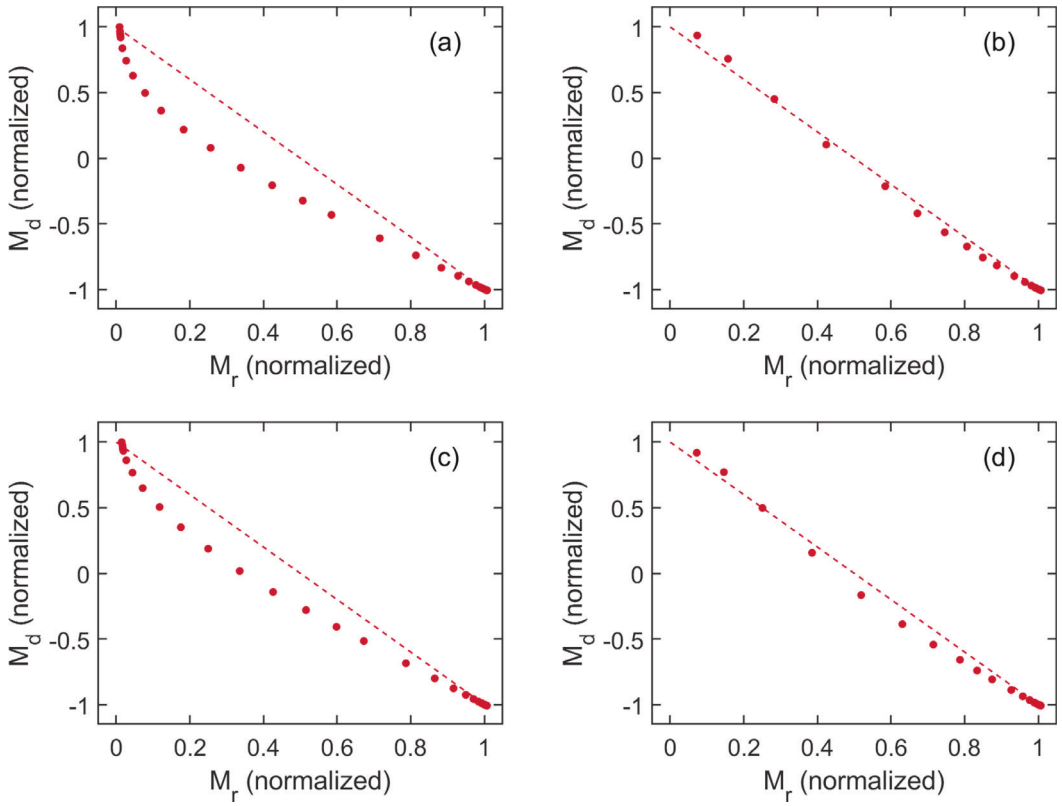

Fig. 7. Uncorrected (left) and corrected (right) Henkel plots correspond to Fig. 4. The magnetite volume fractions are 7.1% [(a) uncorrected and (b) corrected] and 1.4% [(c) uncorrected and (d) corrected]. The red dashed line is the Wohlfarth relation [see (1)].

The mean field (from a single dipole) in the $\hat{z}$-direction on the entire spherical shell is equal to

$$\langle B_z \rangle = \frac{1}{N}\int_0^{\pi} B_z(\theta) dN(\theta) = \frac{\mu_0 m}{8\pi R^3}\cdot \int_0^{\pi} \left[2(\sin(\theta)\cos(\theta))^2 - \sin^4(\theta)\right] d\theta. \quad \text{(A5)}$$

Thus,

$$\langle B_z \rangle = -\frac{\mu_0 m}{64 R^3} < 0. \quad \text{(A6)}$$

So the dipolar interaction is antiferromagnetic (i.e., demagnetizing) on average.

APPENDIX D

The Henkel plots with and without the corrections described in Section IV-C are given in Fig. 7.

ACKNOWLEDGMENT

This work was supported in part by NSF under Grant DMR 1609782 and Grant DMR 2103704, and in part by the

University of Minnesota's Office of Undergraduate Research. The authors especially thank Peat Solheid and the Institute for Rock Magnetism, University of Minnesota, Minneapolis, MN, USA, for the use of their Magnetic Property Measurement System 3 (MPMS 3). They also thank Kevin O'Grady and Liquids Research Ltd., Wales, U.K., http://liquidsresearch.com/, for providing their Series HY Isoparaffin-based Ferrofluid and a critical reading of this article.

REFERENCES

[1] E. P. Wohlfarth, "Relations between different modes of acquisition of the remanent magnetization of ferromagnetic particles," *J. Appl. Phys.*, vol. 29, no. 3, pp. 595–596, Mar. 1958, doi: 10.1063/1.1723232.

[2] S. Thamm and J. Hesse, "The remanence of a Stoner–Wohlfarth particle ensemble as a function of the demagnetisation process," *J. Magn. Magn. Mater.*, vol. 184, no. 2, pp. 245–255, 1998, doi: 10.1016/S0304-8853(97)01135-9.

[3] O. Henkel, "Remanenzverhalten und Wechselwirkungen in hartmagnetischen Teilchenkollektiven," *Phys. Status Solidi, B*, vol. 7, no. 3, pp. 919–929, 1964.

[4] P. E. Kelly, K. O'Grady, P. I. Mayo, and R. W. Chantrell, "Switching mechanisms in cobalt-phosphorus thin films," *IEEE Trans. Magn.*, vol. 25, no. 5, pp. 3881–3883, Sep. 1989, doi: 10.1109/20.42466.

[5] R. W. Chantrell and K. O'Grady, "Magnetic characterization of recording media," *J. Phys. D, Appl. Phys.*, vol. 25, no. 1, pp. 1–23, Jan. 1992, doi: 10.1088/0022-3727/25/1/001.

[6] G. W. D. Spratt, P. R. Brissel, R. W. Chantrell, and E. P. Wohlfarth, "Static and dynamic experimental studies of particulate recording media," *J. Magn. Magn. Mater.*, vol. 75, no. 3, pp. 309–318, 1988, doi: 10.1016/0304-8853(88)90036-4.

[7] P. R. Bissell, R. W. Chantrell, G. J. Tomka, J. E. Knowles, and M. P. Sharrock, "Remanent magnetisation and demagnetisation measurements on particulate recording media," *IEEE Trans. Magn.*, vol. 25, no. 5, pp. 3650–3652, Sep. 1989, doi: 10.1109/20.42389.

[8] F. E. Pinkerton and D. J. Van Wingerden, "Magnetization process in rapidly solidified neodymium-iron-boron permanent magnet materials," *J. Appl. Phys.*, vol. 60, no. 10, pp. 3685–3690, Nov. 1986, doi: 10.1063/1.337576.

[9] M. M. Vopson, "A new method to study ferroelectrics using the remanent Henkel plots," *J. Phys. D, Appl. Phys.*, vol. 51, no. 20, May 2018, Art. no. 205304, doi: 10.1088/1361-6463/aabe16.

[10] J. Freedberg and E. D. Dahlberg, "Effect of demagnetization technique on remanence measurements in metallic ferromagnets," *IEEE Trans. Magn.*, vol. 56, no. 4, pp. 1–4, Apr. 2020, doi: 10.1109/TMAG.2020.2967709.

[11] C. A. M. Vieira *et al.*, "Blocking and remanence properties of weakly and highly interactive cobalt ferrite based nanoparticles," *J. Phys., Condens. Matter*, vol. 31, no. 17, May 2019, Art. no. 175801, doi: 10.1088/1361-648X/ab0353.

[12] J. Garcıa-Otero, M. Porto, and J. Rivas, "Henkel plots of single-domain ferromagnetic particles," *J. Appl. Phys.*, vol. 87, no. 10, pp. 7376–7381, May 2000, doi: 10.1063/1.372996.

[13] Liquids Research Ltd. *Series HY Isoparaffin-Based Ferrofluid*. Bangor, U.K. Accessed: Nov. 82 2021. [Online]. Available: http://liquidsresearch.com/

[14] *Isopar M*, Exxon Mobil Corp., Irving, TX, USA.

[15] *Magnetic Property Measurement System 3*, Quantum Design Inc., San Diego, CA, USA.

[16] *Vibrating Sample Magnetometer Model no. 155*, Princeton Appl. Res., Oak Ridge, TN, USA.

[17] *Confirmed Most of the Particles Would be Superparamagnetic at 77 K Based on the Properties of the Magnetite Particles*. Private Commun. Kevin O'Grady Liquids Res. Ltd., Bangor, U.K.

[18] C. Kittel, *Introduction to Solid State Physics*, 4th ed. Hoboken, NJ, USA: Wiley, 1971, pp. 454–458.